Assessment of Density Functional Methods for Reaction Energetics: Iridium-Catalyzed Water Oxidation as Case Study

Andranik Kazaryan[a] and Evert Jan Baerends[a,b,c]

We investigate basis set convergence for a series of density functional theory (DFT) functionals (both hybrid and nonhybrid) and compare to coupled-cluster with single and double excitations and perturbative triples [CCSD(T)] benchmark calculations. The case studied is the energetics of the water oxidation reaction by an iridium-oxo complex. Complexation energies for the reactants and products complexes as well as the transition state (TS) energy are considered. Contrary to the expectation of relatively weak basis set dependence for DFT, the basis set effects are large, for example, more than 10 kcal mol^{-1} difference from converged basis for the activation energy with 'small' basis sets (DZ/6-31G** for Ir/other atoms, or SVP) and still more than 6 kcal mol^{-1} for def2-TZVPP/6-31G**. Inclusion of the dispersion correction in DFT-D3 schemes affects the energies of reactant complex (RC), TS, and product complex (PC) by almost the same amount; it significantly improves the complexation energy (the formation of RC), but has little effect on the activation energy with respect to RC. With converged basis, some pure GGAs (PBE-D3, BP86-D3) as well as the hybrid functional B3LYP-D3 are very accurate compared to benchmark CCSD(T) calculations. © 2012 Wiley Periodicals, Inc.

Introduction

Density functional theory (DFT) calculations play an important role in the elucidation of reaction mechanisms and in the characterization of transition states and intermediates. In this contribution, we benchmark various DFT methods against reference high level *ab initio* coupled-cluster with single and double excitations and perturbative triples [CCSD(T)] benchmark calculations. This study addresses primarily the convergence of the results with basis set extension but also the choice of DFT functional. It is generally argued that one-electron methods such as DFT and Hartree–Fock (HF) are much less demanding with respect to basis flexibility than correlated methods such as CCSD(T). It is nevertheless known that, due to the variable occupation of the valence *d* orbitals, the treatment of transition metal compounds requires special care in the basis set choice.[1,2] Indeed, we will see that the key energies of our reaction (notably the activation energy) are quite basis set dependent even at the Kohn–Sham DFT level. A basis set such as 6-31G**, often used for computational expediency, severely underestimates (by more than 10 kcal mol^{-1}) the basis set converged activation energy.

System and Computational Details

The O—O bond formation step catalyzed by the [CpIrO(ppy)]$^+$ (ppy = $C_5NH_5C_6H_5$) system is chosen for this case study. This catalyst belongs to the water oxidation catalysts, which are currently receiving much experimental and theoretical interest. An efficient and yet simple iridium-based mononuclear catalyst was synthesized by Bernhard and coworkers[3] A modified

family of 'half-sandwich' pentamethylcyclopentadiene (Cp*) ligated catalysts [Cp*IrO(ppy)]$^+$ (see Fig. 1) was recently synthesized and studied both spectroscopically and theoretically by Crabtree and coauthors.[4–6] The crucial step in the water oxidation catalysis is the formation of an O—O bond, which is believed to take place by bonding of an O of the attacking water molecule (O_w) to the oxo oxygen (O_{oxo}) of the metal–oxo group, involving simultaneous proton transfer (either via a second water molecule to the O_{oxo}[5,7] or from the water molecule to a proton accepting base[8,9] or via a more involved proton relay chain.[10]

For our study, we used both Gaussian-type orbitals (GTOs) with the TURBOMOLE 6.3[11] and NWChem 6.0[12] programs and Slater-type orbitals (STOs) with the program ADF2012.01.[13,14] In the TURBOMOLE DFT calculations, we used the Pople basis sets 6-31G*, 6-31G**, 6-311++G**, and

[a] A. Kazaryan, E. J. Baerends
VU University Amsterdam, Faculty of Exact Sciences, Theoretical Chemistry, De Boelelaan 1083, 1081 HV Amsterdam, The Netherlands

[b] E. J. Baerends
Department of Chemistry, Pohang University of Science and Technology, Pohang 790-784, South-Korea
E-mail: E.J.Baerends@vu.nl

[c] E. J. Baerends
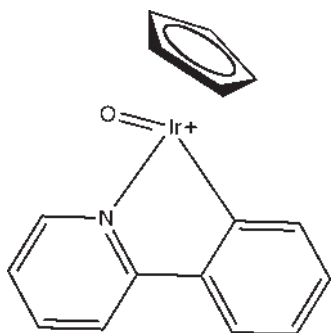*Department of Chemistry, King Abdulaziz University, Jeddah 21589, Saudi Arabia*

Figure 1. Catalyst [CpIrO(ppy)]⁺ (compound **1**).

the Ahlrichs sets (with e.g., [632;321;2] notation standing for a 6s3p2d contraction on iridium, 3s2p1d on C, N, O and 2s on hydrogen):

- double-ζ def2-SV(P): [632;321;2], def2-SVP: [6321;321;21]

- triple-ζ def-TZVP: [633;531;31], def2-TZVP: [6431;5321;31], def2-TZVPP: [64321;5321;321]

- quadruple-ζ basis set def2-QZVPP: [75442;74321;4321].

For iridium, a scalar relativistic effective core potential (ECP) was used for the description of the 60 innermost electrons with the associated basis sets def2-SV(P), def2-SVP, def-TZVP, def2-TZVP, def2-TZVPP, and def2-QZVPP. In combination with Pople basis sets 6-31G** and 6-311++G** for noniridium atoms, we used for iridium the Stuttgart scalar relativistic ECP with double-ζ associated basis set, further denoted as DZ/6-31G** and DZ/6-311++G**. In the calculations with the Amsterdam Density Functional (ADF) code, we used all-electron STO basis sets ranging from DZ/DZ to QZ4P/QZ4P (Ir/rest atoms). Relativistic effects were treated with the scalar zero-order regular approximation.[15,16] The spin-orbit effects have been investigated but did not exceed 1 kcal mol⁻¹.

A variety of popular generalized gradient approximation (GGA) and hybrid exchange-correlation (XC) functionals have been tested. The dispersion corrections were taken into account using the Grimme D3-parametrized XC functionals[17] denoted here by a "-D3" suffix. To judge the quality of the DFT functionals, we need reliable benchmark data. Because the full system [CpIrO(ppy)]⁺+2H$_2$O is too large, we performed CCSD(T) calculations with realistic basis sets on the model system [CpIrO(NH$_3$CH$_3$)]⁺. For completeness, also MP2 and CCSD calculations have been performed, see Supporting Information. All these calculations were carried out using the resolution of identity (RI) approximation as implemented in the ricc2 program of TURBOMOLE package. The errors of RI approximation usually do not exceed 0.1 kcal mol⁻¹[18,19] In these calculations, we used def2-TZVPP, def2-QZVPP/def2-TZVPP, and def2-TZVPP/aug-cc-pVTZ (Ir/rest), with the associated auxiliary basis sets. The core orbitals below −3.0 Hartree (Ir 5s and below) in MP2, CCSD, and CCSD(T) calculations were kept frozen at the self-consistent field (SCF) level (no excitations out of these orbitals). To assess the effect of the frozen core, we carried out a single CCSD(T) calculation with def2-TZVPP basis set with all orbitals correlated. The changes were found to be less than 0.7 kcal mol⁻¹ The T_1 diagnostic showed $\|t_1\|/\sqrt{N_{elect}} \leq 0.017$

which assures a single reference character and thus applicability of CCSD(T) to our systems.[20]

All calculations were performed for the closed shell singlet state.

Results

The specific reaction we are using in these studies is the O—O bond formation step in the water oxidation catalysis catalyzed by the half-sandwich iridium-oxo catalysts [Cp*IrO(ppy)]⁺ which was reported in their recent work by Crabtree and coworkers,[5] following earlier work of Bernhard and coworkers[3]

$$(Ir^V = O)^+ + H_2O \cdots H_2O \rightarrow Ir^{III}(HOOH)^+ \cdots H_2O \qquad (1)$$
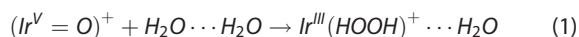
In Ref. [5], the system [CpIrO(ppy)]⁺ (denoted as **1**) was studied theoretically in the gas phase using the B3LYP/DZ/6-31G** approach. To facilitate the proton transfer from the attacking water molecule to the O$_{oxo}$, an additional water molecule was introduced, which is initially [in the reactant complex (RC)] hydrogen bonded to the attacking water molecule, and in the product complex (PC) to the hydrogen peroxide which is coordinated to Ir. The reported structures of the RC, transition state (TS), and PC are shown in Figure 2.† The high reactivity observed in the experiment was ascribed to a moderate activation energy ($\Delta E^\ddagger = (E^{TS} − E^{RC})$ of about 24 kcal mol⁻¹ at B3LYP/6-31G** level. [The TS barrier with respect to the free reactants [Cp*IrO(ppy)]⁺ and water dimer, (H$_2$O)$_2$, was only 8 kcal mol⁻¹.]

In our benchmark study of DFT methods, the relative energies of the structures RC, TS, and PC with respect to **1** and the (H$_2$O)$_2$ dimer (henceforth referred to as the "free reactants") are targeted. The results of single point calculations of the RC, TS, and PC complexes of catalyst **1** with a very large STO basis for the LDA, BLYP, B3LYP functionals are listed in Table 1. The B3LYP/QZ4P/TZ2P STO calculation yields $\Delta E^\ddagger \approx 34$ kcal mol⁻¹. The discrepancy with the value reported in Ref. [5] amounts to roughly 10 kcal mol⁻¹. Such a discrepancy is generally considered too large to be explained by just basis set effects. So we have verified that basis set convergence leads to such a high barrier also with large GTO basis sets of both Pople-type and Ahlrichs-type, see Table 1). The B3LYP activation energies vary substantially on enlarging of the basis set from DZ/6-31G** (21.3 kcal mol⁻¹, close to the value of Ref. [5]) to def2-TZVPP/6-311++G** (33.4 kcal mol⁻¹) and def2-QZVPP (32.5 kcal mol⁻¹). The latter results are comparable with the large basis STO (ADF) result (33.8 kcal mol⁻¹). From table, it is readily seen that even at the def-TZVP level the results are far from converged and only with the def2-TZVPP basis sets one obtains energies comparable with the near limit def2-QZVPP, and the STO QZ4P/TZ2P energies. Other functionals, for example, BLYP and LDA, show similar basis set convergence. In all three considered XC functionals, the def-TZVP basis set is still deficient, it underestimates the activation energy by about

---

†In Ref [5], the structures were denoted C-IN1, C-TS, and C-IN2, respectively.
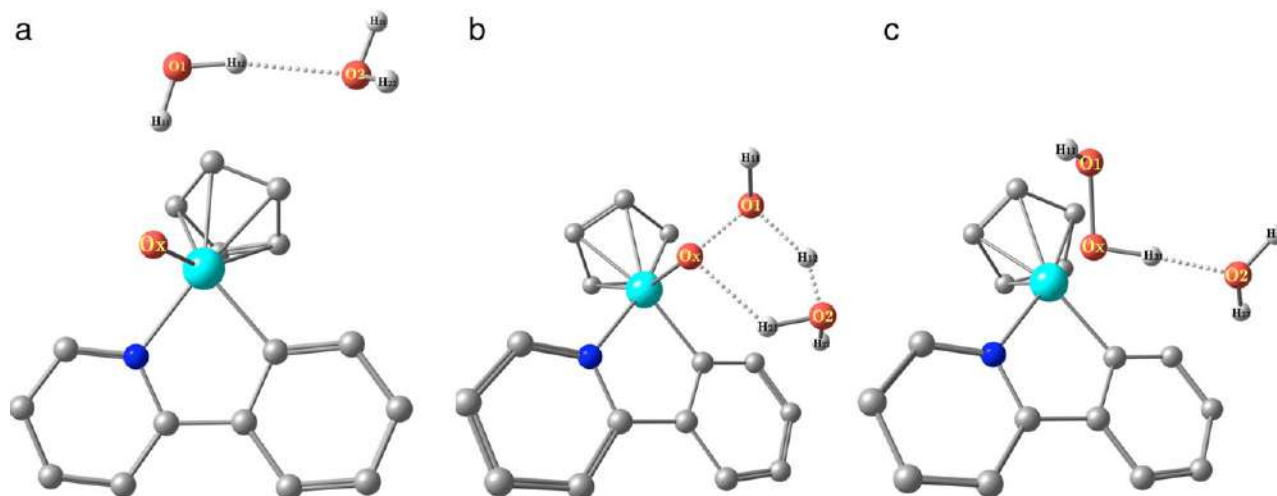
Figure 2. Intermediate structures in the reaction ($Ir^V = O)^+ + H_2O \cdots H_2O \rightarrow Ir^{III}(HOOH)^+ \cdots H_2O$ catalyzed by compound $[CpIrO(ppy)]^+$. Colour code: white—hydrogen grey—carbon, dark blue—nitrogen, red—oxygen and light blue—iridium. The nonwater hydrogens are not shown for clarity. The geometries were obtained from Ref [5].

$6 \div 7$ kcal mol^{-1} compared with the GTO def2-TZVPP basis, which proved with B3LYP to give results reasonably close to those of the large STO QZ4P/TZ2P basis. It should be noted that a balanced basis set should be used. The results in the table demonstrate that a large basis on Ir combined with a more modest basis (6-31G**) on the other atoms leads to an underestimated activation energy as compared to the converged basis set result. A small basis on Ir (e.g., DZ) combined with a large basis on the other atoms (6-311++G**) similarly gives a too low activation energy.

Apart from the basis set convergence, we are interested in the comparison of the (basis set converged) results of the various DFT functionals to benchmark values obtained with a reliable correlated method. The large size of the system prevents, however, application of a high-level treatment such as the CCSD(T) method. We therefore resort to a model system (compound **2**) with the phenyl ring replaced with methyl and pyridine with ammonia ligands as shown in Figure 3.
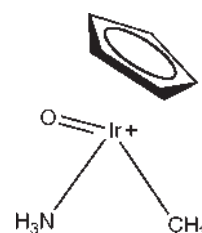
Figure 3. The model system $[CpIrO(NH_3CH_3)]^+$ (compound **2**).

Before discussing the performance of the functionals, we give a more extensive assessment of the basis set effects for the model Ir complex, compound **2**. First, a full geometry optimization has been performed.

To optimize the geometries of the model system, we first made a preliminary selection of an exchange-correlation functional. For this purpose, we carried out single point calculations on the model system using several density functionals and the CCSD(T) method, as explained in Supporting Information.

Using B3LYP-D3 method, a full geometry optimization was performed for the compound **2**, water dimer $(H_2O)_2$, and intermediates of the reaction 1. We locate a TS structure that is similar to the original B3LYP one.[5] These geometries are used in the rest of this work. When reference is made to "compound **2**," the optimized structure of the model complex $[CpIrONH_3CH_3]^+$ is meant. All the structures (water dimer $(H_2O)_2$, compound **2**, RC, TS, and PC) obtained with the B3LYP-D3/def2-TZVPP method are listed in Supporting information. The TS has been characterized with a single imaginary frequency. The compound **2** superimposed with the system **1** is shown in Figure 4. We note that the simplification of the

Table 1. Energies (in kcal/mol) of the reactant complex (RC), transition state (TS), and product complex (PC) structures relative to the free reactants (Ir complex and water dimer); activation energy $\Delta E^{\ddagger} = E_{TS} - E_{RC}$.

Method	STO basis	RC	TS	PC	$\Delta E^{\ddagger}$
LDA[a]	QZ4P/TZ2P	−15.9	2.1	−9.5	18.0
BLYP[a]		−6.5	33.2	12.9	39.7
B3LYP[a]		−7.8	26.0	3.3	33.8
Method	GTO Bases	RC	TS	PC	$\Delta E^{\ddagger}$
LDA[b]	def-TZVP	−19.2	−8.4	−20.2	10.8
	def2-TZVPP	−17.8	−0.7	−12.2	17.2
BLYP[b]	def-TZVP	−9.5	22.1	1.9	31.6
	def2-TZVPP	−8.3	29.7	9.5	38.0
B3LYP[b]	DZ/6–31G**	−16.1	5.3	−14.0	21.3
	def2-TZVPP/6–31G**	−15.3	10.7	−7.9	26.0
	DZ/6–311++G**	−10.0	17.0	−5.8	27.0
	def2-TZVPP/6–311++G**	−9.5	23.9	1.4	33.4
	def-TZVP	−10.4	14.2	−8.4	24.6
	def2-TZVPP	−9.2	22.6	0.2	31.8
	def2-QZVPP/def2-TZVPP	−9.3	22.7	0.3	32.0
	def2-QZVPP	−8.0	24.4	1.8	32.5
B3LYP[c]	DZ/6–31G**	−16.0	8.0	−11.1	24.0

[a] Results were obtained with ADF program. [b] Results were obtained with TURBOMOLE program. [c] G03 results from Ref. [5]. The geometries were obtained from Ref [5]. Basis sets specified at Ir / other atoms.
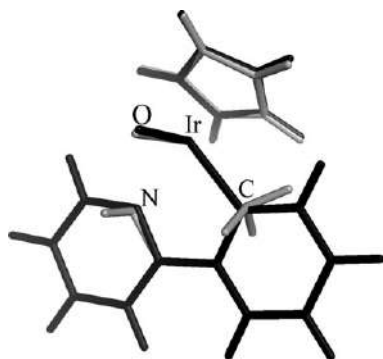
Figure 4. Superimposed structures of compound $[CpIrO(ppy)]^+$ and the model system $[CpIrO(NH_3CH_3)]^+$.

ligands does not lead to any serious distortion of the coordination of the Ir. We therefore trust the model compound **2** to represent faithfully the electronic structure characteristics of the full system **1**. The intermediate and TS structures are very similar to those of compound **1** (see Supporting Information, Fig. S3).

For all the optimized structures, we carried out CCSD(T) calculations with def2-TZVPP and def2-QZVPP/def2-TZVPP basis sets. We note that increasing the basis set on iridium atom in the CCSD(T) calculations from def2-TZVPP to def2-QZVPP yields a change of less than 0.2 kcal mol^{-1}. It was shown in Supporting Information that the use of def2-TZVPP basis set for noniridium atoms is sufficient. The CCSD(T)/def2-QZVPP/def2-TZVPP calculations in Table 2 constitute our reference.

To investigate the basis set convergence for DFT functionals, we used for these structures a variety of GTO and STO bases in combination with B3LYP and BP86 functionals. The energies of the individual species relative to the reactants (compound **2** and water dimer) are listed in Table 2. The errors of the relative energies of the individual species RC, TS, and PC are shown in Figure 5, and the derived quantities such as the activation energy ($\Delta E^{\ddagger} = E^{TS} - E^{RC}$) and the reaction energy ($\Delta H = E^{PC} - E^{RC}$) are shown in Figure 6.

The dependence of the B3LYP results on GTO basis set is considerable. The figure displays two series of GTO basis sets, the Pople sets DZ/6-31G*-def2-TZVPP/6-311++G** and the Ahlrichs sets def2-SV(P) – def2-QZVPP. In each series, it is clear that the smaller sets are far from convergence. The energies of RC, TS, and PC are all too low compared to the CCSD(T) benchmark. For the larger basis sets, the differences with CCSD(T) change sign, and these energies are all higher than the CCSD(T) benchmark values. This is a pattern that is repeated with the STO basis sets. The convergence in the GTO and STO basis sets is toward similar positive values, but the convergence is clearly much faster with the STO basis sets. In fact, only if all atoms including Ir, or just only the other atoms, have the small DZ basis, do we find negative differences with CCSD(T) for the STO basis sets. The deviation from the converged values is particularly large for the Gaussian bases DZ/6-31G*, DZ/6-31G**, and for the def2-SV(P), def2-SVP, and def-TZVP bases. Assuming the STO QZ4P/QZ4P basis to yield the converged basis results, we note that the deviations from

convergence for even the def2-TZVPP/6-31G** basis, which might not be considered really small, amount to -7.8, -14.1, and -10.2 kcal mol^{-1} for RC, TS, and PC energies, respectively. The smaller GTO basis sets give really large discrepancies compared to the converged results.

It is worth noting that the STO basis set convergence is significantly faster. Only the DZ basis is truly deficient, but reasonable behavior is observed with a basis set such as TZP/TZP, and larger than TZP bases (e.g., TZ2P/TZ2P) are almost converged. A slightly more even convergence is seen in pure GGA BP86 results. There is a slight difference in the converged STO compared to GTO values for the PC energies, which translates into a numerical difference of a few kcal mol^{-1} for the reaction energies between converged STO and GTO values.

A cautionary remark should be made regarding the landscapes of the potential energy. The deviations of the energies with the various basis sets are not systematic, for instance when enlarging the basis from DZ/6-31G** to def2-TZVPP/6-311++G** the complexation, activation, and reaction energies increase by 6.8, 12.9, and 9.4 kcal mol^{-1}, respectively. This may have implications for the widely accepted strategy of performing a geometry optimization at, for example, B3LYP/6-31G** level and subsequently refining the energies by single point calculations at a higher level of theory. Although a full investigation of this point is beyond the scope of the present communication, we caution that the potential energy landscape may change unpredictably with respect to too small basis sets, which might jeopardize the mentioned strategy.

We can now use the converged energies for an assessment of the performance of the functionals, which is done in Table 3. The errors of the relative energies are shown in Figures 7 and 8.

To make a survey of different DFT methods, we performed calculations with a few popular GGAs (BLYP, PBE, BP86, OLYP, OPBE, rPBE), some hybrid functionals (B97, B3LYP, B3LYP*, BHandHLYP, OPBE0, PBE0), Meta GGAs (M06-L, TPSS, revTPSS, SSB-D), Meta hybrids (M06, M06-2X, TPSSh), a range-separated (CAM-B3LYP), and a double hybrid (B2PLYP). B3LYP* has a reduced amount of exact exchange (15%)[21] and BHandHLYP has an increased amount (50%). In a number of cases, Grimme's dispersion corrections[17] were added. Both GTOs (with Turbomole) and STOs (with ADF) were used.

The spread of more than 10 kcal mol^{-1} over the DFT functionals in the energies of each of the species (RC, TS, PC) is alarming (see Fig. 7) and demonstrates the necessity of a careful selection of the density functional. If we consider the activation energy, $\Delta E^{\ddagger}$ (see Table 3, Fig. 7), which is our primary target, we note that several GGAs are close to the CCSD(T) benchmark value of 38.2 kcal mol^{-1}: PBE, BP86, and OPBE. Others, such as BLYP, OLYP, and rPBE, are 6–7 kcal mol^{-1} too high. Among the hybrids, only B3LYP and B3LYP* are OK, although a few kcal/mol worse than the mentioned GGAs (we concentrate on the larger STO basis results). The hybrid extension of the GGAs that were already good lead to deterioration in the form of lower activation energies (cf. PBE0, OPBE0). BHandHLYP (more HF exchange) is also inferior to B3LYP (lower activation energy by ca. 7 kcal mol^{-1}). A similar trend is observed in the M06 series[22,23] of MetaGGAs and their hybrid

Table 2. Basis set convergence with GTO and STO bases.

Method	Basis set	RC	TS	PC	$\Delta E^{\ddagger}$	ΔH
CCSD(T)	def2-TZVPP	−12.9	25.4	1.1	38.3	14.1
	def2-QZVPP/def2-TZVPP	−13.0	25.2	1.1	38.2	14.1
B3LYP[a]	DZ/6–31G*	−16.4	11.9	−9.2	28.3	7.2
	DZ/6–31G**	−16.6	11.6	−9.1	28.2	7.5
	def2-TZVPP/6–31G**	−15.7	17.7	−2.4	33.4	13.3
	DZ/6–311++G**	−10.4	23.8	−0.9	34.1	9.4
	def2-TZVPP/6–311++G**	−9.8	31.2	7.0	41.1	16.9
	def2-SV(P)	−17.1	3.8	−17.7	20.8	−0.6
	def2-SVP	−17.2	10.1	−10.2	27.3	7.0
	def-TZVP	−13.2	20.1	−4.1	33.2	9.1
	def2-TZVP	−10.3	27.3	3.6	37.6	13.9
	def2-TZVPP	−9.9	28.7	4.8	38.6	14.7
	def2-QZVPP/def2-TZVPP	−9.9	28.9	5.0	38.8	14.9
	def2-QZVPP	−8.6	30.6	6.5	39.3	15.1
B3LYP[b]	DZ/DZ	−13.7	16.9	−5.3	30.6	8.3
	DZ/DZP	−9.6	26.3	2.6	35.8	12.2
	DZ/TZP	−8.8	27.5	4.7	36.3	13.5
	DZ/TZ2P	−8.6	28.6	5.1	37.2	13.7
	DZ/QZ4P	−7.9	30.8	6.7	38.7	14.6
	TZP/DZ	−13.5	21.2	−1.2	34.8	12.3
	TZP/DZP	−9.4	28.1	4.3	37.4	13.6
	TZP/TZP	−8.8	28.5	5.7	37.3	14.5
	TZP/TZ2P	−8.6	29.5	6.1	38.1	14.8
	TZP/QZ4P	−7.9	30.7	6.4	38.6	14.3
	TZ2P/DZ	−13.7	16.9	−5.3	30.6	8.3
	TZ2P/TZP	−8.8	28.5	5.7	37.3	14.5
	TZ2P/TZ2P	−8.5	31.3	8.2	39.8	16.7
	TZ2P/QZ4P	−7.9	31.8	7.8	39.7	15.6
	QZ4P/DZ	−12.1	28.2	5.7	40.2	17.8
	QZ4P/DZP	−8.8	31.7	8.1	40.5	16.9
	QZ4P/TZP	−8.6	31.1	8.9	39.8	17.5
	QZ4P/TZ2P	−8.3	32.3	8.8	40.6	17.1
	QZ4P/QZ4P	−7.9	31.8	7.8	39.7	15.6
BP86[b]	DZ/DZ	−13.1	17.0	0.3	30.1	13.4
	DZ/DZP	−9.0	25.6	7.3	34.5	16.3
	DZ/TZP	−7.9	27.4	9.9	35.3	17.7
	DZ/TZ2P	−7.7	28.5	10.1	36.2	17.8
	DZ/QZ4P	−7.8	30.2	11.5	38.0	19.2
	TZP/DZ	−13.0	21.1	4.2	34.1	17.2
	TZP/DZP	−8.8	27.4	9.0	36.2	17.8
	TZP/TZP	−7.8	28.4	10.9	36.2	18.7
	TZP/TZ2P	−7.7	29.0	10.6	36.7	18.2
	TZP/QZ4P	−7.5	30.3	11.6	37.9	19.1
	TZ2P/DZ	−13.1	17.0	0.3	30.1	13.4
	TZ2P/TZP	−7.8	28.4	10.9	36.2	18.7
	TZ2P/TZ2P	−7.5	30.9	12.6	38.4	20.2
	TZ2P/QZ4P	−7.4	31.3	12.7	38.7	20.1
	QZ4P/DZ	−12.9	28.4	11.2	41.3	24.1
	QZ4P/DZP	−8.3	30.8	12.5	39.0	20.8
	QZ4P/TZP	−7.6	30.9	13.5	38.5	21.1
	QZ4P/TZ2P	−7.4	31.3	13.0	38.7	20.4
	QZ4P/QZ4P	−7.4	31.3	12.7	38.7	20.1

[a] GTO basis sets (TURBOMOLE program). [b] STO basis sets (ADF program). Energies (in kcal/mol) of the reaction intermediates for the reaction of water with the model compound $[CplrO(NH_3CH_3)]^+$ relative to the free reactants (Ir complex and water dimer); activation $\Delta E^{\ddagger} = E_{TS} - E_{RC}$ and reaction $\Delta H = E_{PC} - E_{RC}$ energies. The geometries are always the fully optimized ones at B3LYP-D3/def2-TZVPP level.

within 1.3 kcal mol^{-1}: 0.0 (TPSS), −1.3 (TPSSh), and −0.6 (revTPSS). We conclude that for the activation energy several functionals perform quite well.

For the complexation energy in the formation of the RC (benchmark value −13.0 kcal mol^{-1}), the behavior of the functionals is somewhat different. None of the pure GGAs is very close, their complexation energies are typically 6–7 kcal mol^{-1} too weak, that is, not sufficiently negative (binding). This suggests that for those for which the activation energies ($\Delta E^{\ddagger} = E^{TS} - E^{RC}$) were good, the TS energies have similar deviation, see the $\Delta\Delta E_{TS}$ results (gray columns) in Figure 7. Addition of the dispersion correction corrects the complexation energy in many cases to approximately the right value. The effect is that the $\Delta\Delta E_{TS}$ results improve considerably in Figure 7 when the D3 correction is added (compare PBE with PBE-D3, BP86 with BP86-D3, B3LYP with B3LYP-D3, TPSS with TPSS-D3). This holds for all functionals, both for those with good and for those with somewhat poor activation energies (the D3 correction is so designed). Because the dispersion correction lowers the total energy by an amount that is roughly proportional to the number of atom–atom pairs, the D3 correction at a given functional is about the same in RC and TS, and the activation energy changes rather little (see Fig. 8), as also observed by Siegbahn et al.[26] and (with a somewhat larger effect on the activation energy) by Mulholland and coworkers[27] The functionals PBE-D3 and B86-D3 therefore give good complexation energies and continue to give good activation energies (OPBE-D3 was not available). BLYP-D3 and rPBE-D3 give good complexation energies, but still not good activation energies (OLYP-D3 was not available). The hybrid functionals PBE0 and B3LYP (also B3LYP*) have somewhat smaller discrepancy in the complexation energy, and also a smaller D3 correction. The D3 addition corrects the complexation energy to about the right value, and again does not change the activation energy much, which remains somewhat poor for PBE0-D3 and good but not excellent for B3LYP-D3. We note that the OPTX-based functionals OPBE and OLYP have the weakest complexation energies for RC, but still the activation energy is good for OPBE (not for OLYP: 8 kcal mol^{-1} too high). The SSB-D functional,[28] a MetaGGA extension of the SSB-sw (based on switching between the PBE and OPBE functionals) with the added Grimme dispersion correction, gives an excellent complexation energy ($\Delta\Delta E_{RC} \approx 0.0$ kcal mol^{-1}) while also yielding reasonable activation and reaction energies (within 3.6 kcal mol^{-1}).

The energies for the PC seem to be the most difficult to get right, they show for many functionals considerable deviation
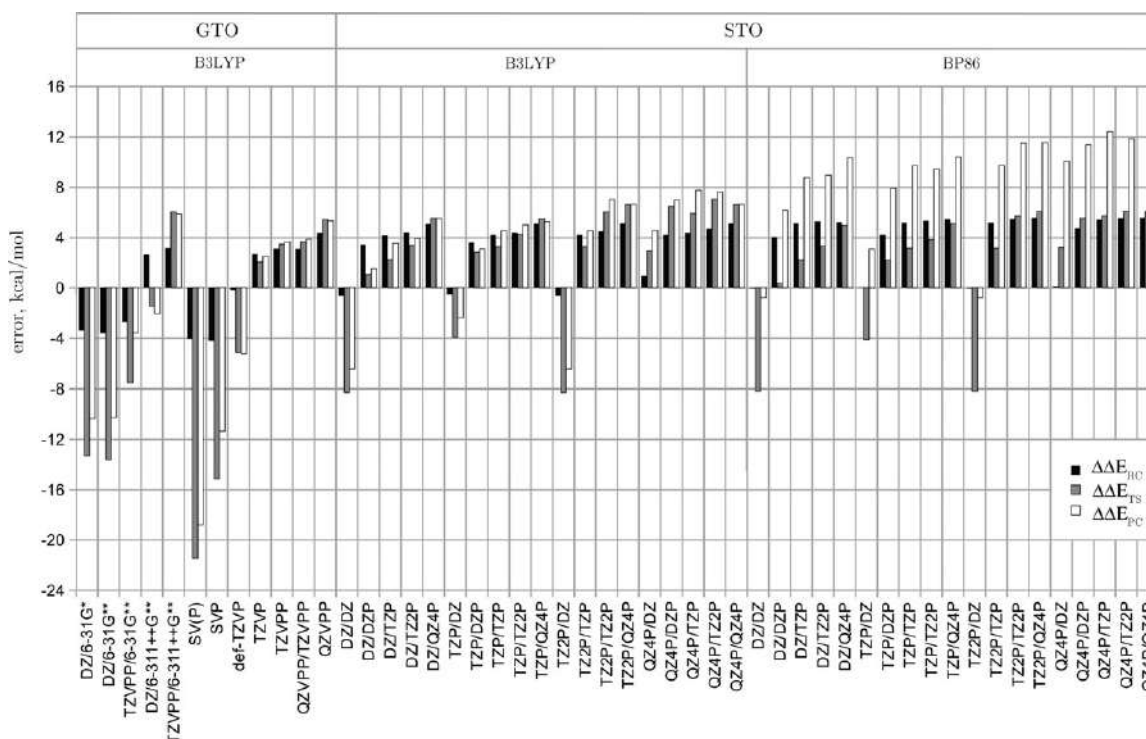
extensions [M06-L(0%HF), M06(27%HF), M06-2X(54%HF)]. Although M06-L yields an activation energy close to the benchmark value ($\Delta\Delta E^{\ddagger} \approx 1.8$ kcal mol^{-1}), M06 and M06-2X underestimate the barrier by about 2.7 and 11.3 kcal mol^{-1}, respectively. In the Meta GGA class, the TPSS functionals[24,25] are very good, they match our benchmark activation barriers

Figure 5. Basis set dependence of relative energies (with respect to the free Ir complex and water dimer) of the reactant complex (RC), transition state (TS), and product complex (PC) of the model system $[CpIrO(NH_3CH_3)]^+$ (**2**). The deviations from the corresponding reference CCSD(T) values are depicted. For simplicity, the 'def2-' prefixes in the Ahlrichs basis sets are omitted, only 'def-' prefixes are retained.
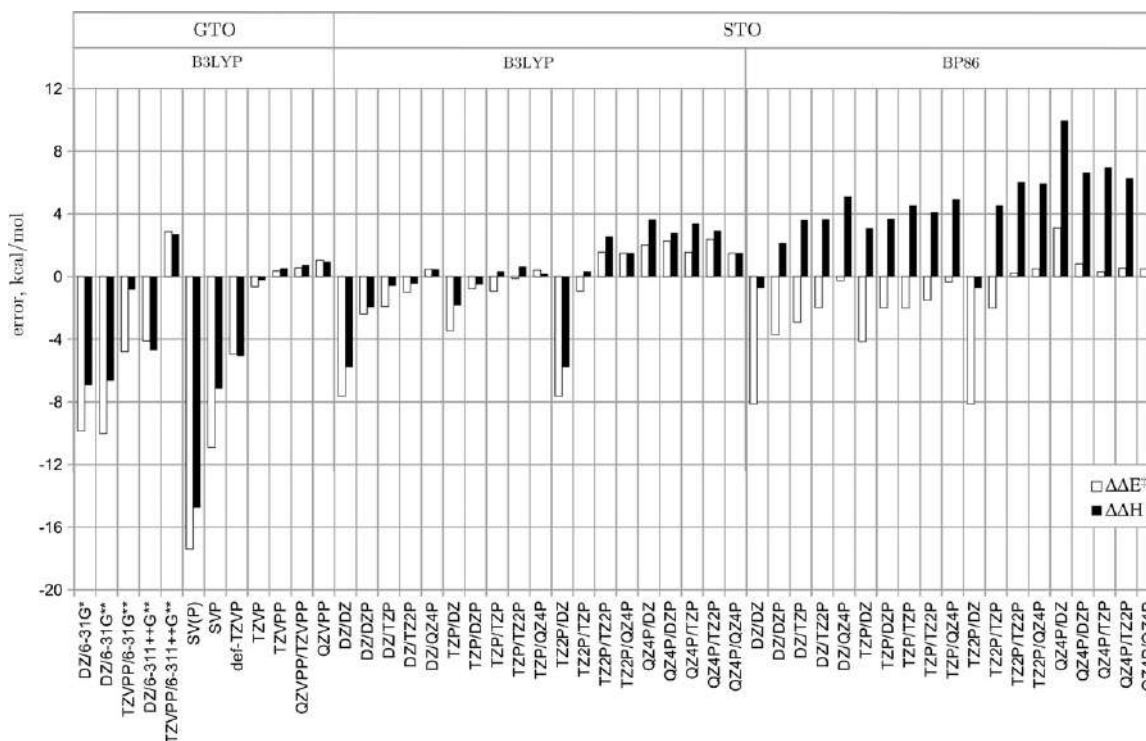
Figure 6. Basis set dependence of the error of the activation energy ($\Delta E^{\ddagger} = E^{TS} - E^{RC}$) and reaction energy ($\Delta H = E^{PC} - E^{reactants}$) in the reaction catalyzed by the model system $[CpIrO(NH_3CH_3)]^+$ (**2**). The error is relative to the corresponding CCSD(T) results. For simplicity, the 'def2-' prefixes in the Ahlrichs basis sets are omitted, only 'def-' prefixes are retained.

Table 3. Comparison between functionals.

Method	GTO Basis	RC	TS	PC	$\Delta E^{\ddagger}$	ΔH
CCSD(T)	def2-TZVPP	−12.9	25.4	1.1	38.3	14.1
	def2-QZVPP/def2-TZVPP	−13.0	25.2	1.1	38.2	14.1
B3LYP	def2-TZVPP	−9.9	28.7	4.8	38.6	14.7
	def2-QZVPP	−8.6	30.6	6.5	39.3	15.1
B3LYP-D3	def2-TZVPP	−14.0	24.5	0.9	38.5	15.0
	def2-QZVPP	−12.8	26.4	2.6	39.2	15.4
B97	def2-TZVPP	−7.4	36.0	13.8	43.4	21.1
	def2-QZVPP	−6.1	38.0	15.5	44.1	21.6
B97-D3	def2-TZVPP	−13.0	30.5	8.9	43.5	21.9
	def2-QZVPP	−11.7	32.5	10.6	44.2	22.3
B2PLYP	def2-TZVPP	−11.5	33.0	9.2	44.5	20.7
	def2-QZVPP	−13.0	32.4	8.6	45.4	21.6
B2PLYP-D3	def2-TZVPP	−13.7	30.7	7.2	44.5	20.9
	def2-QZVPP	−12.6	32.8	9.0	45.4	21.6
CAM-B3LYP[a]	def2-TZVPP	−11.6	20.8	−3.0	32.3	8.6
	def2-QZVPP	−10.2	22.7	−1.4	32.9	8.8

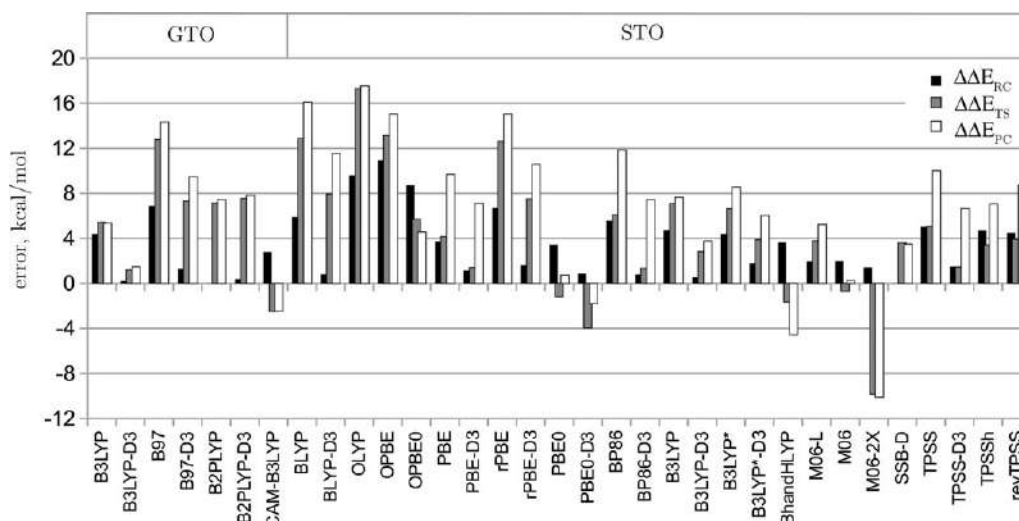| Method	STO Basis	RC	TS	PC	$\Delta E^{\ddagger}$	ΔH
BLYP	QZ4P/TZ2P	−7.1	38.1	17.2	45.2	24.3
BLYP-D3		−12.2	33.1	12.6	45.4	24.9
OLYP		−3.4	42.5	18.7	45.9	22.1
OPBE		−2.1	38.3	16.2	40.4	18.2
OPBE0		−4.3	30.9	5.7	35.2	10.0
PBE		−9.3	29.4	10.8	38.7	20.1
PBE-D3		−11.9	26.6	8.2	38.5	20.1
rPBE		−6.3	37.9	16.2	44.2	22.5
rPBE-D3		−11.4	32.7	11.7	44.1	23.1
PBE0		−9.6	24.0	1.9	33.6	11.4
PBE0-D3		−12.2	21.2	−0.7	33.4	11.5
BP86		−7.4	31.3	13.0	38.7	20.4
BP86-D3		−12.2	26.6	8.6	38.8	20.8
B3LYP		−8.3	32.3	8.8	40.6	17.1
B3LYP-D3		−12.5	28.0	4.9	40.5	17.4
B3LYP*		−8.6	31.8	9.7	40.5	18.3
B3LYP*-D3		−11.2	29.1	7.1	40.3	18.4
BhandHLYP		−9.4	23.5	−3.5	32.9	5.9
M06-L		−11.1	29.0	6.4	40.1	17.4
M06		−11.0	24.5	1.4	35.5	12.4
M06–2X		−11.6	15.4	−9.0	26.9	2.6
M06-HF		−11.6	−0.3	−23.1	11.3	−11.6
SSB-D		−13.0	28.8	4.6	41.8	17.6
TPSS		−8.0	30.3	11.1	38.3	19.1
TPSS-D3		−11.5	26.7	7.8	38.2	19.3
TPSSh		−8.3	28.6	8.2	36.9	16.5
revTPSS		−8.5	29.1	9.8	37.6	18.4

[a] CAM-B3LYP results were obtained with NWChem[12] program.
Energies (in kcal/mol) of the reaction intermediates for the reaction of water with the model compound [CpIrO(NH$_3$CH$_3$)]$^+$ relative to the free reactants (Ir complex and water dimer); activation $\Delta E^{\ddagger} = E_{TS} - E_{RC}$ and reaction $\Delta H = E_{PC} - E_{RC}$ energies. The geometries are always the fully optimized ones at B3LYP-D3/TZVPP level. GTO basis results from Turbomole, STO basis results from ADF.

and $\Delta\Delta H$ (Fig. 8) to very similar errors for all three systems, RC, TS, and PC (Fig. 7). PBE0 and PBE0-D3 are the best for the PC energy, but are too deficient in the activation energy.

Conclusions

In conclusion, in the present study, we highlighted the basis set dependence of DFT calculations, which appears to be considerable for the type of reaction (metal–oxo catalyzed O—O bond formation) studied here. Even though the basis set dependence of this one-electron method (molecular orbital method) is not as strong as the one of correlated *ab initio* methods, it still has to be taken into account. Notably, basis sets of double-ζ quality (e.g., 6-31G**) prove too small for reliable results, yielding discrepancies of more than 10 kcal mol^{-1} with converged results, which is unacceptable for reactivity studies (barrier heights in particular). The minimum reasonable GTO basis set for the DFT calculations on the considered systems is shown to be a triple-ζ basis of the def2-TZVPP quality on all atoms. These basis set effects are not particular for the system investigated here. Our motivation for this case study has been the occurrence of discrepancies of large basis set calculations with published smaller basis set results in other cases, which met with disbelief at the referees. In a recent study of O—O bond formation catalyzed by an iron-based complex, Ertem et al.[30] have similarly cautioned against the unexpectedly large functional and basis set effects that may occur. In agreement with the recent report on the study of multiplet states of transition metal complexes,[31] a faster convergence of DFT energies with STO basis sets as compared to the GTO sets was observed. With converged basis sets, we validated various exchange-correlation functionals for the description of the O—O bond formation step of water oxidation catalyzed by the iridium–oxo compound **1** and the truncated model compound **2**. The results were supported by highly correlated *ab initio* CCSD(T) results. For the important activation energy, it was found that the pure GGA functionals PBE and BP86 (and their D3 variants) provide a very accurate description (within 1 kcal mol^{-1} from the reference CCSD(T) values). The same holds for TPSS(-D3). Several functionals deviate only a few kcal/mol: OPBE, B3LYP(-D3), M06-L, SSB-D, TPSSh, and revTPSS. When also good complexation energies, both for the reactants and the products complex, are required, the dispersion correction becomes indispensable (although it has little effect on the activation energy). As good compromise functionals—good activation barrier, good reactants complexation energy, not too bad products complex

from the target value of 1.1 kcal mol^{-1}. The GGA and hybrid GGA functionals that would emerge as best candidates from the evaluation above (PBE-D3, BP86-D3, and B3LYP-D3) are among those with the smallest discrepancies for $\Delta\Delta E_{PC}$ (but still 7.1, 7.5, and 3.8 kcal mol^{-1}, respectively). In view of the importance of a reliable $\Delta\Delta E^{\ddagger}$, the GGA functionals PBE-D3, BP86-D3 therefore remain the ones to be recommended for studies of the type of reaction we are considering here (oxidation with metal-oxo compounds), which is in accord with the previously found good performance of these methods.[29] Among the hybrids B3LYP-D3, M06 and TPSSh can be recommended, where TPSSh owes its good performance for $\Delta\Delta E^{\ddagger}$

Figure 7. XC functional dependence of relative energies ΔE (with respect to the free Ir complex and water dimer) of the reactant complex (RC), transition state (TS), and product complex (PC) of the model system $[CpIrO(NH_3CH_3)]^+$ (**2**). The deviations $\Delta\Delta E$ from the corresponding reference CCSD(T) values are depicted. The GTO series was obtained with the def2-QZVPP and the STO with QZ4P/TZ2P (Ir/rest) basis sets.

energy—PBE-D3, BP86-D3, and TPSS-D3 emerge. The hybrid functionals B3LYP-D3 and TPSSh also give very good results (both a few kcal mol^{-1} worse for the activation energy, but clearly better for the PC energy). M06-L and SSB-D (somewhat too high activation energies but good RC energies), finally, are overall pretty good, without a big failure for any of the three investigated energies. The performance of DFT functionals for the C—H hydroxylation reaction (the H abstraction step) with a metal-oxo compound (Fe(IV)O^{2+}), which has strong electronic analogy to the present reaction, has recently been scrutinized by Chen et al.[32] These authors found—with def2-TZVPP single point calculations at def2-TZVP optimized geometries—that B3LYP and B3LYP-D3 consistently underestimate the reaction barrier by more than 10 kcal mol^{-1}, whereas the pure GGAs BP86 and PBE have smaller errors but still underestimate considerably. On the basis of our investigation, we feel that these discrepancies cannot be attributed to basis set defi-

ciency. The results are less favorable for the DFT functionals than we have obtained here. This may be related to the fact that our systems are singlet states, whereas those in Ref. [32] are quintet and triplet states. The B3LYP functional is known to favor high spin states as was recently demonstrated by Bowman and Jakubikova.[33] From this point of view, the GGAs BP86 and PBE seem to be somewhat more reliable 'all-round' functionals.

We emphasize that it is not the purpose of this work to further elucidate the experimental findings for the specific reaction studied. From our study, one may infer that the high reactivity established experimentally[5] with the catalyst **1** cannot be rationalized in terms of low activation energies in the O—O bond formation with just a gas-phase study. The energy barriers found in this study would be prohibitive for the reaction. A possible rationale for the high reactivity may be related to the solvent effects, and of course, free energies of activation would be needed. An extensive study using explicit solvent
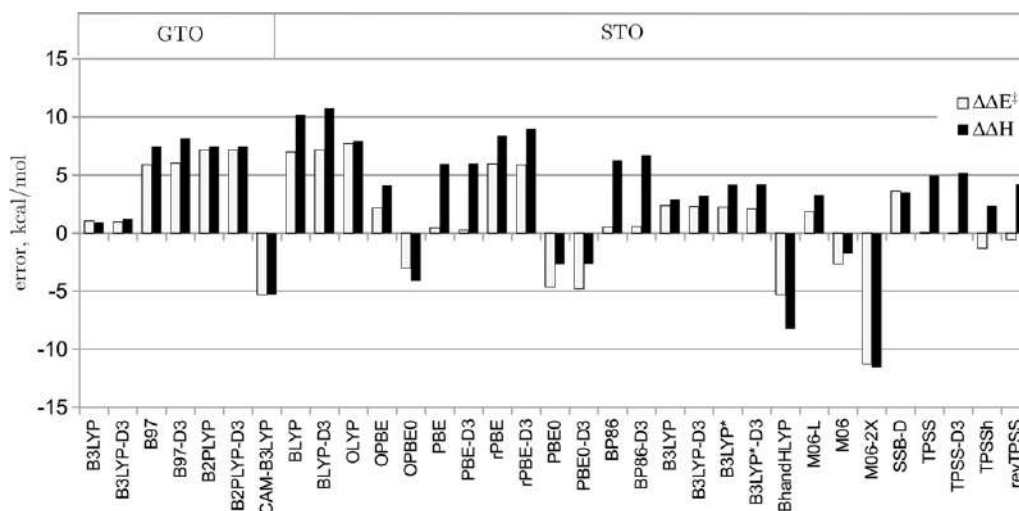
Figure 8. Activation ($\Delta E^{\ddagger} = E^{TS} - E^{RC}$) and reaction $\Delta H = E^{PC} - E^{reactants}$ energies relative to the benchmark CCSD(T) results for the model system $[CpIrO(NH_3CH_3)]^+$ (**2**). The GTO series was obtained with the def2-QZVPP and the STO with QZ4P/TZ2P (Ir/rest) basis sets.

effects and free energies of activation, for instance by thermo-dynamic integration in an AIMD study, is therefore deemed necessary.

Acknowledgments

[1] J. W. Richardson, W. C. Nieuwpoort, R. R. Powell, W. F. Edgell, *J. Chem. Phys.* **1962,** *36,* 1057.

[2] M. Piacenza, I. Hyla-Kryspin, S. Grimme, *J. Comput. Chem.* **2007,** *28,* 2275.

[3] N. D. McDaniel, F. J. Coughlin, L. L. Tinker, S. Bernhard, *J. Am. Chem. Soc.* **2008,** *130,* 210.

[4] F. Hull, D. Balcells, J. D. Blakemore, C. D. Incarvito, O. Eisenstein, G. W. Brudvig, R. H. Crabtree, *J. Am. Chem. Soc.* **2009,** *131,* 8730.

[5] J. D. Blakemore, N. D. Schley, D. Balcells, J. F. Hull, G. W. Olack, C. D. Incarvito, O. Eisenstein, G. W. Brudvig, R. H. Crabtree, *J. Am. Chem. Soc.* **2010,** *132,* 16017.

[6] N. D. Schley, J. D. Blakemore, N. K. Subbaiyan, C. D. Incarvito, F. D'Souza, R. H. Crabtree, G. W. Brudvig, *J. Am. Chem. Soc.* **2011,** *133,* 10473.

[7] J. L. Vallés-Pardo, M. C. Guijt, M. Iannuzzi, K. S. Joya, H. J. M. de Groot, F. Buda, *ChemPhysChem.* **2012,** *13,* 140.

[8] Z. Chen, J. J. Concepcion, X. Hu, W. Yang, P. G. Hoertz, T. J. Meyer, *Proc. Natl. Acad. Sci.* **2010,** *107,* 7225.

[9] L.-P. Wang, Q. Wu, T. Van Voorhis, *Inorg. Chem.* **2010,** *49,* 4543.

[10] R. Bianco, P. J. Hay, J. T. Hynes, *J. Phys. Chem. A* **2011,** *115,* 8003.

[11] TURBOMOLE V6.3 2011, a development of University of Karlsruhe and Forschungszentrum Karlsruhe GmbH, 1989–2007, TURBOMOLE GmbH, since 2007; available at: http://www.turbomole.com.

[12] M. Valiev, E. Bylaska, N. Govind, K. Kowalski, T. Straatsma, H. V. Dam, D. Wang, J. Nieplocha, E. Apra, T. Windus, W. de Jong, *Comput. Phys. Commun.* **2010,** *181,* 1477.

[13] E. J. Baerends, D. E. Ellis, P. Ros, *Chem. Phys.* **1973,** *2,* 41.

[14] G. Te Velde, F. M. Bickelhaupt, E. J. Baerends, C. F. Guerra, S. J. A. van Gisbergen, *J. Comput. Chem.* **2001,** *22,* 931.

[15] E. van Lenthe, E. J. Baerends, J. G. Snijders, *J. Chem. Phys.* **1994,** *101,* 9783.

[16] E. van Lenthe, R. van Leeuwen, E. J. Baerends, J. G. Snijders, *Int. J. Quantum. Chem.* **1996,** *57,* 281.

[17] S. Grimme, J. Antony, S. Ehrlich, H. Krieg, *J. Chem. Phys.* **2010,** *132,* 154104.

[18] K. Eichkorn, O. Treutler, H. Ohm, M. Haser, R. Ahlrichs, *Chem. Phys. Lett.* **1995,** *242,* 652.

[19] F. Weigend, M. Haser, *Theor. Chem. Acc.* **1997,** *97,* 331.

[20] T. J. Lee, P. R. Taylor, *Int. J. Quantum. Chem.* **2009,** *36,* 199.

[21] M. Reiher, O. Salomon, B. Artur Hess, *Theor. Chem. Acc.* **2001,** *107,* 48.

[22] Y. Zhao, D. G. Truhlar, *J. Chem. Phys.* **2006,** *125,* 194101.

[23] Y. Zhao, D. Truhlar, *Theor. Chim. Acta* **2008,** *120,* 215–241.

[24] J. Tao, J. P. Perdew, V. N. Staroverov, G. E. Scuseria, *Phys. Rev. Lett.* **2003,** *91,* 146401.

[25] V. N. Staroverov, G. E. Scuseria, J. Tao, J. P. Perdew, *J. Chem. Phys.* **2003,** *119,* 12129.

[26] P. E. M. Siegbahn, M. R. A. Blomberg, S.-l. Chen, *J. Chem. Theory Comput.* **2010,** *6,* 2040.

[27] R. Lonsdale, J. N. Harvey, A. J. Mulholland, *J. Phys. Chem. Lett.* **2010,** *1,* 3232.

[28] M. Swart, M. Sola, F. M. Bickelhaupt, *J. Chem. Phys.* **2009,** *131,* 094103.

[29] W. Hujo, S. Grimme, *Phys. Chem. Chem. Phys.* **2011,** *13,* 13942.

[30] M. Z. Ertem, L. Gagliardi, C. J. Cramer, *Chem. Sci.* **2012,** *3,* 1293.

[31] M. Swart, *J. Chem. Theory Comput.* **2008,** *4,* 2057.

[32] H. Chen, W. Lai, S. Shaik, *J. Phys. Chem. Lett.* **2010,** *1,* 1533.

[33] D. N. Bowman, E. Jakubikova, *Inorg. Chem.* **2012,** *51,* 6011.

Assessment of Density Functional methods for reaction energetics: Iridium catalyzed water oxidation as case study

Andranik Kazaryan[a] and Evert Jan Baerends[a,b,c] *

[a] *VU University Amsterdam, Theoretical Chemistry, De Boelelaan 1083, 1081 HV Amsterdam, The Netherlands,* [b] *Dep. of Chemistry, Pohang University of Science and Technology, Pohang 790-784, South-Korea,* [c]*Dep. of Chemistry, King Abdulaziz University, Jeddah 21589, Saudi Arabia*

E-mail: a.k.kazaryan@gmail.com,E.J.Baerends@vu.nl

---

*To whom correspondence should be addressed

October 27, 2012

To test different density functionals for the description of the reaction catalyzed by compound **1**
Figure 1 (see main text) we need benchmark energies obtained with a high-level correlated method
such as CCSD(T).
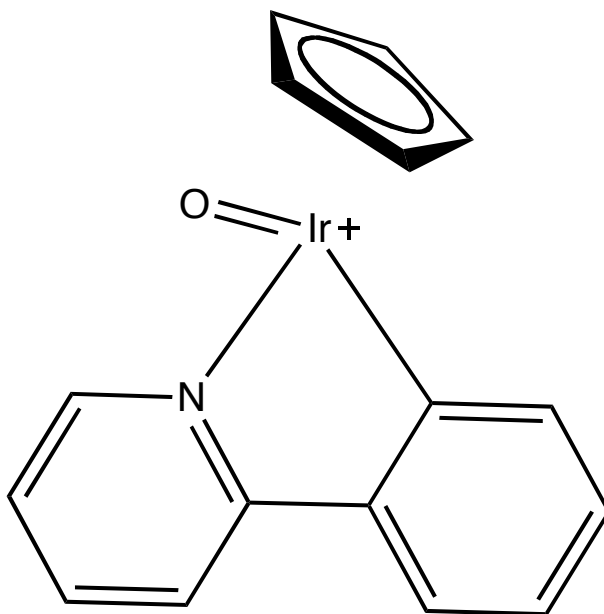

Figure 1: Catalyst $[CpIrO(ppy)]^+$ (compound **1**).

Since the size of the system **1** is too large to apply CCSD(T) method, we resort to a model system (compound **2**) with the phenyl ring replaced with methyl and pyridine with ammonia ligands as shown in Figure 2.
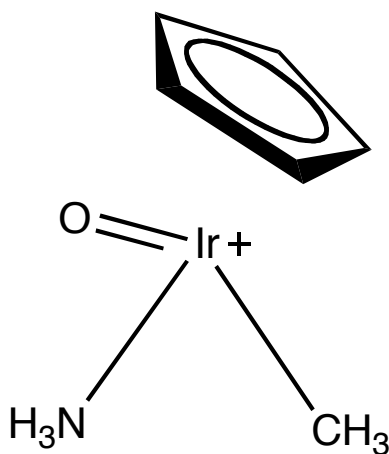

Figure 2: The model system $[CpIrO(NH_3CH_3)]^+$ (compound **2**).

The substituted ligands were optimized (i.e. the C-H and N-H bonds and angles of the $CH_3^{\cdot}$ radical and the NH_3 molecule) with the rest of the system kept rigid (i.e. the Ir-C, Ir-N and Ir-O distances as well as the angles). This procedure was followed for all complexes (RC, TS and PC).

Before carrying out a full geometry optimization a preliminary choice of exchange-correlation functional is performed. To this end single point energies were calculated at the MP2, CCSD, CCSD(T) and DFT levels. The results are listed in Table 1. To assess the error introduced by the frozen core orbitals in these correlated methods, we, in addition, performed fully correlated MP2, CCSD and CCSD(T) calculations with def2-TZVPP basis set (denoted as def2-TZVPP' in Table 1). The effect appears to be moderate, $0.2 \div 0.7$ kcal mol^{-1}. In addition to the def2-TZVPP basis set we also employed def2-TZVPP/aug-cc-pVTZ (Ir/rest) which yields similar (difference $\leq$ 1.0 kcal mol^{-1}) energies in MP2 and CCSD calculations. The use of def2-TZVPP/aug-cc-pVTZ for CCSD(T) was computationally not feasible. Nonetheless, the CCSD results suggest that the def2-TZVPP is already a reasonable basis for both iridium and non-iridium atoms in the CCSD(T) calculations. It is readily seen that MP2, while yielding quite good complexation energy for RC, fails completely to describe the activation and reaction energies. The CCSD values underestimate the activation and reaction energies by ca. 5 kcal mol^{-1}, while giving good complexation energy, underestimating it by only 1.0 kcal mol^{-1}. We will use the CCSD(T)/def2-TZVPP calculations as benchmark.

The GGAs with the exception of the BLYP functional give good activation energies, as does B3LYP. The RC energies are within $1.4 \div 3.4$ kcal mol^{-1} (less binding), whereas the energies of the product complex deviate more strongly: $0.2 \div 8$ kcal mol^{-1} (less binding). In each instant the inclusion of the dispersion corrections make the RC's more binding, but they overcorrect, making the energies too strongly binding (too negative) by ca. 1 kcal mol^{-1}. PBE-D3, BP-D3 and B3LYP-D3 give all quite good agreement (roughly at the 1 kcal/mol level, with the CCSD(T)/def2-TZVPP values, B3LYP-D3 being clearly the best for the energy of the product complex PC.

Based on the above results we chose PBE-D3, BP86-D3 and B3LYP-D3 functionals to optimize the geometry of model **2**. We performed full geometry optimization (lifting the constraints on the

Table 1: Energies (kcal/mol) of the reactant complex (RC), transition state (TS) and product complex (PC) structures of the model system $[CpIrO(NH_3CH_3)]^+$ relative to the free reactants (Ir complex and water dimer); activation $\Delta E^{\ddagger} = E_{TS} - E_{RC}$ and reaction $\Delta H = E_{PC} - E_{RC}$ energies. The model compound $[CpIrO(NH_3CH_3)]^+$ was obtained from the full system $[CpIrO(ppy)]^+$ by substituting the phenyl ring with methyl and pyridine with ammonia ligands and a subsequent optimization of the substituents while the rest of the system was kept rigid (see text for details).

Method	Basis set	RC	TS	PC	$\Delta E^{\ddagger}$	ΔH
	def2-TZVPP	-13.9	46.2	16.5	60.0	30.4
MP2[a]	def2-TZVPP'[b]	-14.1	45.5	15.8	59.5	29.9
	def2-TZVPP/ATZ[c]	-13.8	46.6	17.5	60.4	31.3
	def2-TZVPP	-11.7	24.2	-6.7	35.9	5.1
CCSD[a]	def2-TZVPP'[b]	-11.9	23.5	-7.4	35.4	4.5
	def2-TZVPP/ATZ[c]	-11.8	24.2	-6.2	36.0	5.6
CCSD(T)[a]	def2-TZVPP	-13.1	27.6	-0.9	40.7	12.1
	def2-TZVPP'[b]	-12.9	28.3	-0.3	41.1	12.6
PBE		-11.5	29.4	5.8	40.9	17.3
PBE-D3		-14.1	26.4	3.2	40.5	17.3
BLYP		-9.0	38.1	12.6	47.2	21.6
BLYP-D3	QZ4P/TZ2P[d]	-14.0	32.2	7.9	46.2	21.9
BP		-9.5	31.8	8.3	41.2	17.8
BP-D3		-14.1	26.2	3.8	40.3	17.9
B3LYP		-9.8	32.1	4.0	41.9	13.8
B3LYP-D3		-13.9	27.3	-0.1	41.2	13.8

[a] GTO basis (TURBOMOLE program). [b] The prime indicates that all electrons have been correlated, unlike the unprimed results, where the core orbitals have been treated as inert. [c] ATZ is a shorthand for aug-cc-pVTZ. [d] STO basis (ADF program).

Ir-ligand bond distances and angles mentioned before) using TURBOMOLE at the PBE-D3/def2-TZVPP, BP86-D3/def2-TZVPP and B3LYP-D3/def2-TZVPP levels on system **2**. Using the GGA functionals, however, we were not able to locate the TS geometries resembling the one identified with the B3LYP functional in the full system, which features a ring structure O_{oxo}-O_{w1}-H-O_{w2}-H-O_{oxo} (see Figure 3b of the main text). Therefore, in the further calculations (see main text) we only use the geometries optimized at B3LYP-D3/def2-TZVPP level. These structures are shown in Figure 3 and the cartesian coordinates are listed below.

(a) Reactants complex (RC)   (b) Transition state (TS)   (c) Product complex (PC)
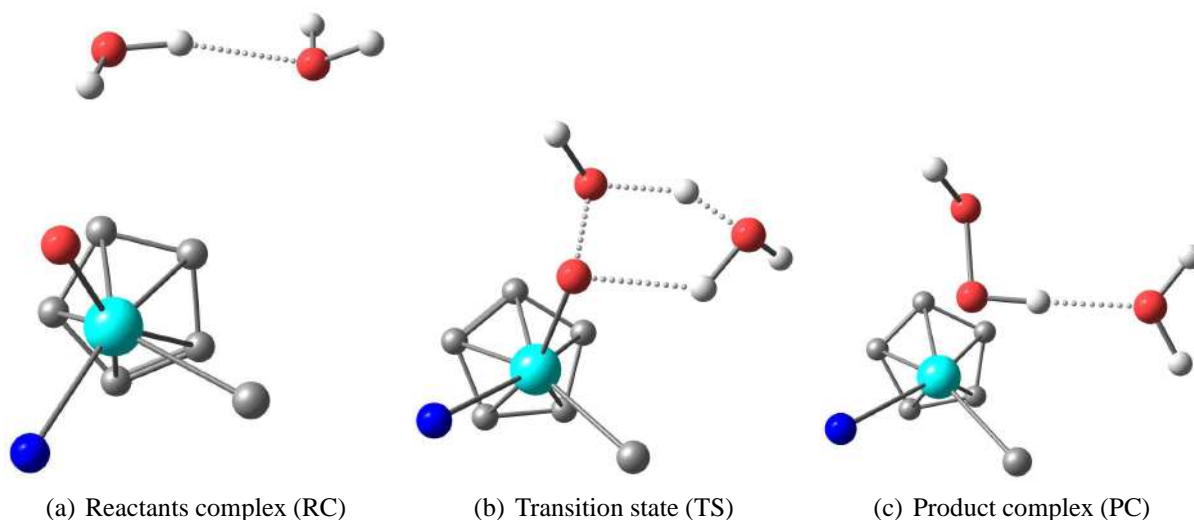
Figure 3: Intermediate structures in the reaction of water with the model compound $[CpIrO(NH_3CH_3)]^+$. Colour code: white - hydrogen grey - carbon, dark blue - nitrogen, red - oxygen and light blue - iridium. The non-water hydrogens are not shown for clarity. All geometries are fully optimized at B3LYP-D3/def2-TZVPP level.

B3LYP-D3/def2-TZVPP optimized geometries and total energies of the free reactants and reaction intermediates for the reaction of water with the model compound $[CpIrO(NH_3CH_3)]^+$.

```
Water dimer
6
-152.86864107
O          -0.0872926    0.0374733    1.5605784
H           0.0489690   -0.0098543    0.6030629
H           0.7396716   -0.2616446    1.9455364
O           0.0690530   -0.0189177   -1.3509279
H          -0.1631845    0.8649984   -1.6508337
H          -0.6489234   -0.5858810   -1.6480569
```

Catalyst **2**
20
-469.24445160

Ir	0.0287032	-0.0746555	-0.0068884
O	0.1223469	-0.0307077	1.7655701
N	2.1630119	-0.0072560	0.2810295
C	0.3423066	1.9220210	-0.6745748
C	-0.3129553	-1.1928980	-2.0628333
C	-1.1381837	-0.0717396	-2.0747460
C	-0.6516998	-1.9765673	-0.9003357
C	-2.0125869	-0.1237804	-0.9210211
C	-1.7620232	-1.3393372	-0.2382929
H	-2.2665011	-1.6889483	0.6483801
H	-1.1015562	0.7327637	-2.7898509
H	0.4627578	-1.4255036	-2.7737309
H	-0.2099549	-2.9229563	-0.6298199
H	-2.7720950	0.5987742	-0.6696360
H	2.2400617	0.1201516	1.2936976
H	2.6449893	0.7539986	-0.1897722
H	2.6325411	-0.8733053	0.0325770
H	-0.5970826	2.4106264	-0.9064320
H	0.7948107	2.3952457	0.1948354
H	1.0145877	1.9513663	-1.5277483

Reactant complex (RC)
26
-622.13546830

Ir	0.0879425	1.0599534	0.0483264
C	1.7650667	0.2511237	-1.3936602
C	1.2157894	-0.8561084	-0.7498694
C	2.2498215	1.1495857	-0.3758739
C	1.3413353	-0.6783668	0.6840600
C	2.0503911	0.5262066	0.9094518
O	0.9841672	0.9974302	3.6691412
C	-1.5203871	-0.2101976	-0.5228287
N	-1.0236111	2.5126933	-1.0970551
O	-0.5597216	2.0911685	1.3509085
H	2.2780582	0.9253569	1.8879640
H	0.7298619	-1.6868937	-1.2334806
H	1.7964978	0.4249461	-2.4567162
H	2.7545006	2.0863974	-0.5540845
H	1.0076496	-1.3589405	1.4540028
H	0.2877011	1.5042637	3.2319946
H	0.6094589	0.1209663	3.8268194
O	0.3789587	-1.8960620	3.6546651
H	-0.4327628	-2.2699509	4.0126273
H	1.0843761	-2.2683778	4.1947534
H	-0.4323613	3.1462551	-1.6271353
H	-1.7204050	2.1328505	-1.7321866
H	-1.4924021	3.0505960	-0.3636347
H	-1.4429828	-1.1773881	-0.0393603
H	-2.3893778	0.3220461	-0.1405879
H	-1.5761751	-0.3191614	-1.6024242

Transition state (TS)
26
-622.07411521

Ir	0.0875057	-0.1310061	0.7354062
C	0.6840005	-1.7626536	2.0476142
C	-0.7342211	-1.7431080	1.9053616
C	1.0744020	-0.5734334	2.7817828
C	-1.2134927	-0.4993861	2.4333889
C	-0.0737054	0.1897512	3.0049763
O	-0.7547731	2.7472614	0.9001787
C	-0.9325384	-0.7249752	-1.0187191
N	1.7900861	0.0773905	-0.6019372
O	-0.2425088	1.7666416	-0.1021537
H	-0.1051660	1.1589642	3.4754892
H	-1.3335252	-2.5158676	1.4526035
H	1.3330635	-2.5749456	1.7639909
H	2.0783427	-0.3105457	3.0721510
H	-2.2455546	-0.2079250	2.5361224
H	-0.1953809	3.5213147	0.7365094
H	-1.9887910	2.7576203	0.2753957
O	-2.5984068	2.3576007	-0.5441160
H	-3.3551629	1.8340936	-0.2459073
H	-1.8469757	1.7536988	-0.8387079
H	1.6719051	-0.4579291	-1.4576755
H	2.6687133	-0.2089820	-0.1829547
H	1.8760861	1.0569953	-0.8650001
H	-0.8436470	0.0232191	-1.8154575
H	-1.9938572	-0.8955791	-0.8242786
H	-0.5306992	-1.6614075	-1.4113651

9

Product complex (PC)
26
-622.11161463

Ir	0.8379654	0.0634183	-0.1253897
C	2.0049813	0.5558841	-1.8586625
C	2.0565391	-0.8603828	-1.6383531
C	2.7306314	1.1918841	-0.7708003
C	2.6710763	-1.0841202	-0.3735199
C	3.1192578	0.2013204	0.1309757
O	1.1931508	-0.3299981	2.9012261
C	-0.8726018	-1.0782091	-0.6225683
N	-0.6180153	1.6546198	0.1075600
O	0.1317871	-0.3363999	1.9099938
H	3.6138574	0.3604058	1.0750218
H	1.6520381	-1.6154749	-2.2924793
H	1.6340603	1.0440338	-2.7450623
H	2.8973074	2.2512516	-0.6607692
H	2.8658763	-2.0420741	0.0792960
H	0.7887805	0.1974173	3.6064587
H	-0.4242685	-3.3906051	2.8215658
O	-0.8069490	-2.7411017	2.2236506
H	-1.1995853	-3.2233603	1.4892504
H	-0.2162646	-1.2742760	1.9995188
H	-1.4115527	1.5256468	-0.5141729
H	-0.9818791	1.6515723	1.0577902
H	-0.2399028	2.5794152	-0.0709701
H	-1.6702515	-0.9729971	0.1204613
H	-1.2788591	-0.7623323	-1.5854008
H	-0.6199797	-2.1359166	-0.7084162